

NEW RESULTS ON THE HADRONIC AND SEMILEPTONIC DECAYS OF  
CHARMED  $D$  MESONS MEASURED IN  $e^+e^-$  COLLISIONS<sup>†</sup>

Rafe H. Schindler  
California Institute of Technology  
Pasadena, California 91125 U.S.A.

representing  
The MARK III COLLABORATION<sup>††</sup>

ABSTRACT

We present a high statistics study of the hadronic and semi-leptonic decays of  $D^0$  and  $D^+$  charmed mesons collected at the  $\Psi(3770)$  in the MARK III magnetic detector at the  $e^+e^-$  storage ring SPEAR.

Introduction

Early theoretical ideas on charmed meson decay centered around the Spectator Model, wherein the light quark plays no role in the decay. The models of charmed meson decay have evolved in an attempt to explain the early experimental data which emerged from  $e^+e^-$  collisions. The current theoretical understanding of weak  $D$  decays, hinges on three measurements all having large uncertainties:

- 1) The difference in lifetimes of the  $D^0$  and  $D^+$ :<sup>[1]</sup>  
 $(\tau^+/\tau^0) \sim 2.4.$
- 2) The observation of certain two-body hadronic decays:<sup>[2]</sup>  
 $\Gamma(D^0 \rightarrow \bar{K}^0\pi^0)/\Gamma(D^0 \rightarrow K^-\pi^+) = .75 \pm .35.$
- 3) The deviations among Cabibbo suppressed hadronic decays of the  $D^0$ :<sup>[3]</sup>  
 $\Gamma(D^0 \rightarrow \pi^+\pi^-) \neq \Gamma(D^0 \rightarrow K^+K^-)$

Accurate measurements of the  $D^0$  and  $D^+$  lifetimes (item 1) influences our understanding of the  $D$  decay mechanism. Because the leptonic width of the  $D$  is negligible, and the semileptonic partial widths of the  $D^0$  and  $D^+$  should be nearly equal,\* a difference in lifetimes implies a difference in the non-leptonic widths of the two states. Numerous theoretical solutions have been proposed to either enhance the  $D^0$  or suppress the  $D^+$  non-leptonic width to account for the difference. These ideas generally predict certain patterns among exclusive decays of the  $D$ , and provide a way of distinguishing the underlying process. Some examples of these ideas are described below.

Several authors have noted that QCD corrections to the weak Hamiltonian provide a small non-leptonic enhancement both to  $D^+$  and  $D^0$ .<sup>[4]</sup> A difference can arise, however, if interference is permitted among the  $D^+$  spectator diagrams which lead to identical final states (Fig. 1a).<sup>[5]</sup> The color structure in these models leads to the definite prediction of a strong suppression of certain exclusive decays such as  $D^+ \rightarrow \bar{K}^0\pi^0$  and  $D^+ \rightarrow \phi\pi^+$  (item 2). It has been argued that soft gluon exchange may provide a means of removing the color suppression. The presence of non-spectator processes, which contribute to the  $D^0$  and not the  $D^+$  (at the Cabibbo allowed level), would also lead to a difference in

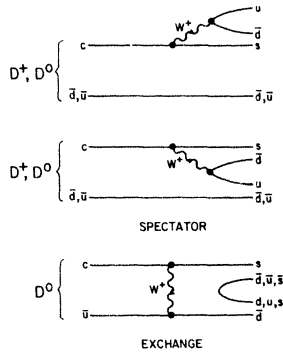


Figure 1a,b

lifetimes. An example is the W-exchange graph (Fig. 1b) which leads to pure  $I = 1/2$  final states of the  $D^0$ .<sup>[5,6]</sup> These diagrams are generally ignored because they are suppressed by helicity at the light quark vertex ( $\propto M_q^2/M_c^2$ ), and by the small probability of annihilation (overlap) ( $\propto f_b^2/M_c^2$ ).<sup>[6,7]</sup> It is argued that the existence of spin 1 color octet-gluons in the  $D^+$  wave function, or the radiation of octet-gluons from the light quark, may relax this suppression.<sup>[7]</sup> The observation of the decays  $D^0 \rightarrow \bar{K}^0 K^0$  or  $D^0 \rightarrow \bar{K}^0 \phi$  would provide direct evidence for

<sup>†</sup>Work supported by the U.S. Department of Energy, Contract No. DE-AC03-81-ER40050.

<sup>††</sup>See A. Seiden, these proceedings.

\*Non-spectator  $D^+$  graphs may enter, but are Cabibbo suppressed.<sup>[14]</sup>

this process, since they occur predominantly through non-spectator graphs<sup>\*\*</sup>.<sup>[8]</sup> W-exchange dominance would also relax the color suppression of  $D^0 \rightarrow \bar{K}^0\pi^0$ .

The third item addresses our knowledge of the Kobayashi Maskawa (KM) weak mixing matrix, since exact SU(3) predicts these partial widths to be equal within small phase space corrections.<sup>[9]</sup> Differences could arise either from SU(3) violations, or problems with the KM mixing angles. That the larger deviation was observed in the  $K^+K^-$  rate, measuring the ordinary Cabibbo angle, favors the former explanation. The long  $b$  lifetime ( $\sim 10^{-12}$  sec) also favors this explanation. Additional measurements are necessary to establish the exact magnitude of the discrepancy, both in  $\pi^+\pi^-$  and  $K^+K^-$ . The pattern of  $D^+$  suppressed channels would also help distinguish these two possibilities.

From this discussion, it is clear that many avenues are available to understand the underlying mechanism of  $D$  meson decays, by utilization of both the hadronic decays and the semileptonic decays.

Detector and Data Sample

The data comes from a sample of hadronic events collected at the peak of the  $\Psi(3770)$  resonance, with the MARK III detector at SPEAR. The integrated luminosity of the sample is  $\sim 8100$  nb<sup>-1</sup>. The  $\Psi(3770)$  is associated with the  $^3D_1$  state of the charmonium system. It is thought to decay primarily to  $D^0\bar{D}^0$  and  $D^+D^-$  pairs, providing an enhancement in the hadronic cross section of  $\sim 7$  nb.<sup>[10]</sup> The  $D^0$  and  $D^+$  being pair produced, emerge with fixed momenta (275 and 237 MeV/c, respectively) providing a kinematic constraint that can be utilized in the reconstruction of  $D$  decays.

The MARK III is a solenoidal detector optimized for the study of these decays at SPEAR energies.<sup>[11]</sup> A brief description of the detector follows. A particle emerging from the beam intersection point first traverses a .056" Beryllium vacuum pipe, and a low mass cylindrical trigger chamber containing four axial planes. The central drift chamber contains 30 planes arranged in 5 axial and 2 non-axial groups. With 240  $\mu$ m spatial resolution, in a .41 T field, the chamber provides  $\sim 2\%$  resolution at 1 GeV over 85% of  $4\pi$  sr. Forty-eight axially oriented time-of-flight (TOF) counters with 190 ps resolution are located just outside the drift chamber. Over .76 of  $4\pi$  sr, the TOF counters provide  $2\sigma$  pion-kaon separation up to 1 GeV, and electron-pion separation up to 0.3 GeV. Immediately beyond the TOF counters, and before the magnet coil, is a 12 rl gas sampling calorimeter covering 95% of  $4\pi$  sr. Read out in 12 longitudinal depth samples, it has  $\leq 10$  mr angular resolution, and an energy resolution of  $18\%/\sqrt{E}$ . The photon efficiency is  $>75\%$  at 75 MeV and 100% at 100 MeV.

Non-leptonic Decays

To identify hadronic decays of the  $D$  which are Cabibbo allowed, the kinematics of  $D$  pair production is exploited. Tracks originating from the intersection point are identified as kaons and pions by TOF. Particles lacking TOF information are assumed to be pions. Appropriately charged combinations of tracks are formed, and are constrained to have the beam energy ( $E_{beam}$ ). The small spread in  $E_{beam}$ , and the low momentum of the  $D$  ( $P_D$ ) relative to  $E_{beam}$  leads to a mass resolution of  $\sim 2.5$  MeV. For decays with  $\pi^0$ 's or  $\eta^0$ 's, a two constraint fit is performed.

TABLE I

Channel	Signal	$\epsilon$	This Expt.	MKII <sup>2</sup>	LGW <sup>12</sup>	$Br$ (%) <sup>*</sup>
			$\sigma_B$ (nb)	$\sigma_B$ (nb)	$\sigma_B$ (nb)	
$K^-\pi^+$	889 ± 35	.47	$.28 \pm .01 \pm .03$	$.24 \pm .02$	$.25 \pm .05$	$3.7 \pm 0.6 \pm 0.7$
$\bar{K}^0\pi^0$	281 ± 22	.09	$.40 \pm .04 \pm .03$	$.30 \pm .08$	$.46 \pm .12$	$5.3 \pm 0.9 \pm 0.9$
$K^-\pi^+\pi^0$	810 ± 62	.21	$.53 \pm .05 \pm .10$	$.68 \pm .23$	$1.40 \pm .60$	$7.1 \pm 1.2 \pm 1.7$
$K^-\pi^+\pi^-\pi^0$	1016 ± 44	.23	$.56 \pm .03 \pm .06$	$.68 \pm .11$	$.36 \pm .10$	$7.5 \pm 1.2 \pm 1.4$
$\bar{K}^0\pi^+\pi^-\pi^0$	126 ± 22	.02	$.76 \pm .16 \pm .13$	—	—	$10.2 \pm 2.6 \pm 2.3$
$\bar{K}^0\pi^+$	142 ± 14	.12	$.15 \pm .02 \pm .01$	$.14 \pm .03$	$.14 \pm .05$	$2.5 \pm 0.5 \pm 0.4$
$K^-\pi^+\pi^+$	1085 ± 41	.32	$.42 \pm .02 \pm .04$	$.38 \pm .05$	$.36 \pm .06$	$7.0 \pm 1.1 \pm 1.3$
$\bar{K}^0\pi^+\pi^0$	186 ± 23	.05	$.45 \pm .07 \pm .07$	$.78 \pm .48$	—	$7.6 \pm 1.6 \pm 1.8$
$\bar{K}^0\pi^+\pi^-\pi^0$	187 ± 23	.06	$.38 \pm .05 \pm .04$	$.51 \pm .18$	—	$6.3 \pm 1.3 \pm 1.2$
$K^-\pi^+\pi^+\pi^0$	154 ± 30	.07	$.26 \pm .06 \pm .04$	—	—	$4.3 \pm 1.0 \pm 1.5$

<sup>\*</sup>Assumes  $\sigma(D^+) = 6.0 \pm 0.9 \pm 1.0$  nb  $\sigma(D^0) = 7.5 \pm 1.1 \pm 1.2$ . This is an average of the values given in Table II for CB and Mark II data (see [10]).

<sup>\*\*</sup>OZI-suppressed spectator decays may also occur at a smaller rate.<sup>[7]</sup>

Figures 2a-j show the mass distributions ( $M_{bc}$ ) for ten Cabibbo allowed decays of the  $D^0$  and  $D^+$ . Two of these modes:  $D^0 \rightarrow \bar{K}_s^0 \pi^+ \pi^-$ , and  $D^+ \rightarrow K^- \pi^+ \pi^+$  were previously unseen. Table I summarizes these decays.

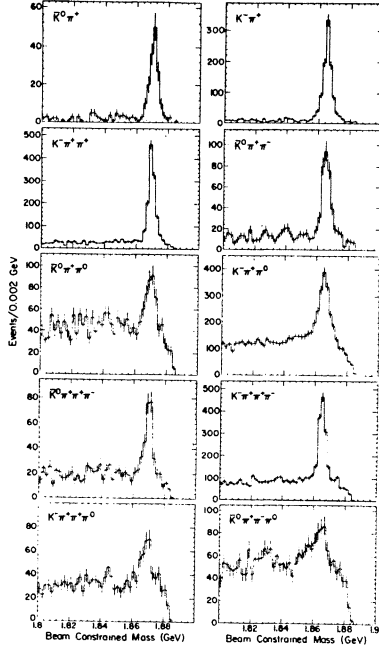


Figure 2a-j

In Table I we compare this experiment with the values obtained by the Lead Glass Wall experiment,<sup>[10]</sup> and by the MARK II.<sup>[2,12]</sup> Agreement is generally satisfactory in all modes, although a precise comparison is difficult since  $\sigma_D$  is varying over the resonance. The large improvement in  $\pi^0$  efficiency, and the greater solid angle coverage, provides significantly better measurements of the decays  $K^- \pi^+ \pi^0$  and  $\bar{K}_s^0 \pi^+ \pi^0$ , as well as allowing the observation of the higher multiplicity decays.

#### Absolute Branching Ratios

While  $\sigma Br$  are well measured for many decay channels the determination of branching ratios requires a knowledge of  $\sigma_D$ . This was previously determined by fitting the shape of the  $\Psi(3770)$  resonance to determine the enhancement due to charm production over the continuum. Assumptions about resonance shape and the division of phase space lead to large systematic errors, as seen in Table II.

TABLE II

	MKII <sup>2,10</sup>	CB <sup>10</sup>	LGW <sup>10</sup>	
$E_{cm}$	$\sqrt{s} = 3.771$	$\sqrt{s} = 3.771$	$\sqrt{s} = 3.774$	GeV
$\sigma(D^0)$	$8.0 \pm 1.0 \pm 1.2$	$6.8 \pm 1.2$	$11.5 \pm 2.5$	nb
$\sigma(D^+)$	$6.0 \pm 0.7 \pm 1.0$	$6.0 \pm 1.1$	$9.1 \pm 2.0$	nb

With this experiment's large sample of detected  $D$  mesons and the knowledge that  $D\bar{D}$  production is taking place, it is possible to derive absolute branching ratios (and hence  $\sigma_D$ ) by counting fully reconstructed events. An event is called "singly" or "doubly" tagged, if one or both  $D$ 's are reconstructed, respectively. The channels  $D^0 \rightarrow K^- \pi^+$  and  $D^+ \rightarrow K^- \pi^+ \pi^+$  are selected for their large signal to background ratios. The branching ratio is computed by evaluating the ratio of single to double tag events:

$$N(\text{singles}) = N(D_{\text{produced}}) \times Br(D \rightarrow \text{tag}) \times \epsilon(\text{tag})$$

$$N(\text{doubles}) = N(\text{singles}) \times Br(\bar{D} \rightarrow \text{tag}) \times \epsilon(\text{recoil tag})$$

After a single tag is found the double tag events are selected by requiring a zero net charge, a recoil momentum within 50 MeV of the expected momentum, and an invariant mass after  $\pi$ - $K$  assignment, close to the  $D$  mass, (to exclude Cabibbo suppressed decays). Figures 3a and 3b show the beam constrained mass of the tags versus the recoils. In each case, a clean signal for double tags is observed. A uniform background from random combinations of tracks, and continuum production, is expected.

TABLE III

Channel	Singles	Doubles	Background	$\epsilon$ (recoil)	$Br$ (%)
$D^0 \rightarrow K^- \pi^+$	$978 \pm 33$	$29 \pm 6$	1.7	.61	$4.9 \pm 0.9 \pm 0.5$
$D^+ \rightarrow K^- \pi^+ \pi^+$	$1109 \pm 37$	$46 \pm 7$	2.2	.45	$9.1 \pm 1.5 \pm 0.9$

Table III summarizes the number of single and double tags, and the resulting branching ratios. These branching fractions contain *no* assumptions about production, and have errors dominated solely by statistics and small uncertainties in

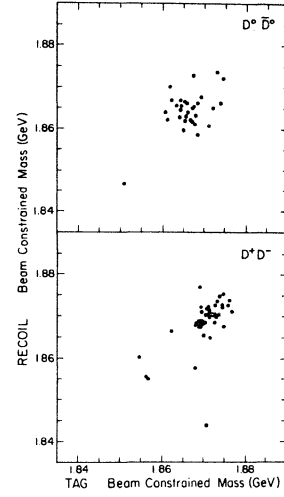


Figure 3a,b

the reconstruction efficiency. They are to be compared to the values in Table I,  $3.7 \pm 0.6 \pm 0.7\%$  and  $7.0 \pm 1.1 \pm 1.3\%$  for  $Br(K^- \pi^+)$  and  $Br(K^- \pi^+ \pi^+)$ , respectively, derived assuming an average cross section of 7.5 nb and 6.0 nb for  $D^0$  and  $D^+$ . Combining Table I and Table III, we independently obtain the production cross sections:

$$\sigma(D^0) = 5.7 \pm 1.1 \pm 0.9 \quad \sigma(D^+) = 4.6 \pm 0.8 \pm 0.7 \text{ nb}$$

The errors on this measurement are still comparable to those in Table II. The central values appear about 20% smaller than the values in Table II, suggesting a systematic reduction in the normalization for  $\sigma_D$ .

#### Rare Non-Leptonic Decays

The decay  $D^0 \rightarrow \bar{K}^0 \pi^0$  is of particular theoretical interest since it measures the degree of "color suppression" present. Figure 4 shows the decay  $D^0 \rightarrow \bar{K}_s^0 \pi^0$ , where we observe  $68 \pm 11$  events, corresponding to:

$$\sigma Br(D^0 \rightarrow \bar{K}_s^0 \pi^0) = .097 \pm .017 \pm .015.$$

We measure the ratio of partial widths:

$$\Gamma(D^0 \rightarrow \bar{K}^0 \pi^0) / \Gamma(D^0 \rightarrow K^- \pi^+) = .35 \pm .07 \pm .07.$$

The previous measurement ( $9 \pm 4$  events) was  $0.75 \pm .35$  for the ratio.<sup>[2]</sup> A value of 0.5 is predicted for pure  $I = 1/2$  final states. Assuming exact SU(3), this decay measures the magnitude of the ratio of two of the three invariant amplitudes present for pseudoscalar-pseudoscalar  $D^0$  decays:<sup>[9]</sup>  $\Gamma(D^0 \rightarrow \bar{K}^0 \pi^0) / \Gamma(D^0 \rightarrow K^- \pi^+) = (1/2) |B/A|^2$ . Under exact SU(3) the value for the ratio implies  $|B| \approx (.84 \pm .14) |A|$ .

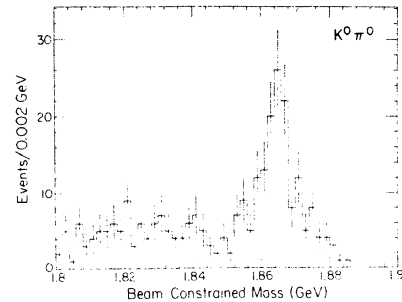


Figure 4

Assuming OZI-violating decays are negligible, the two decays  $D^0 \rightarrow \bar{K}^0 \phi^0$  and  $D^0 \rightarrow \bar{K}^0 K^0$  can only occur through  $W$ -exchange (see Fig. 1b). Because of  $\pi \leftrightarrow K$  misidentification, the mass cannot be calculated using the beam constraint; rather, the usual invariant mass is used. We utilize the knowledge of the  $D$  momentum to reduce background. In Figure 5a we require the  $D$  to be within 50 MeV of the expected momentum, and plot  $M_{K^+ K^-}$ . We observe  $12 \pm 4$  events at the  $D$  mass, with the expected resolution. To test the hypothesis  $D^0 \rightarrow \bar{K}^0 \phi^0$ ,  $M_{K^+ K^-}$  is plotted versus  $M_{K^+ K^-}$  in Figure 5b, after the momentum cut. The  $\phi$  mass resolution is  $\sim 4$  MeV, indicating no more than 4 events are consistent with the  $K_s^0 \phi^0$  hypothesis.

Assuming no events are  $K_s^0 \phi^0$ , then we obtain:

$$\sigma Br(D^0 \rightarrow \bar{K}^0 K^0) = 0.085 \pm 0.028 \pm 0.008 \text{ nb.}$$

This is about 1/5 the rate for  $D^0 \rightarrow K^- \pi^+ \pi^-$ . Assuming 4 events come from  $\bar{K}^0 \phi^0$ , we obtain:

$$\sigma Br(D^0 \rightarrow \bar{K}^0 \phi^0) < 0.13 \text{ nb at 95\% CL.}$$

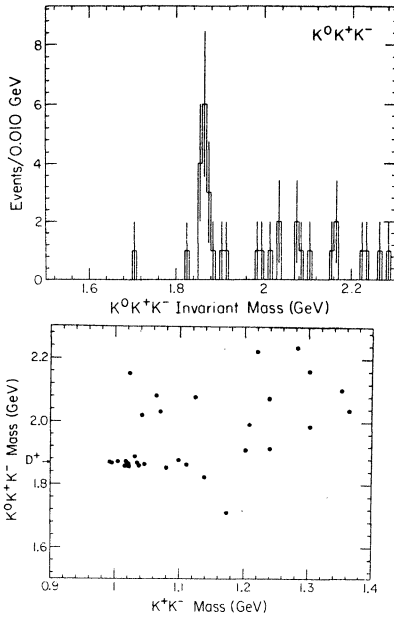


Figure 5a,b

P-wave phase space strongly suppresses this decay relative to other decays such as  $\bar{K}^0 \rho^0$  by a factor of  $\sim 4.6$ . Theoretical calculations suggest a relative branching ratio of  $\sim 20\%$ . Our preliminary measurement of  $\sigma \cdot Br(D^+ \rightarrow \bar{K}^0 \rho^0) = .07 \pm .02$ . Hence, we cannot rule out the presence of W-exchange by our measurement. The concentration of events at low  $M_{K^+ K^-}$  also suggests the possible interpretation of  $D^+ \rightarrow K^+ \delta^0$ , with  $\delta^0 \rightarrow K^+ K^-$ .

We have searched for the Cabibbo suppressed decay  $D^+ \rightarrow \bar{K}^0 K^+$ . We observe 1 event consistent with this decay and set a limit:

$$\Gamma(D^+ \rightarrow \bar{K}^0 K^+)/\Gamma(D^+ \rightarrow K^+ K^-) < 0.11 \text{ at } 95\% \text{ CL.}$$

This is smaller than the ratio for  $D^+ \rightarrow K^+ K^-$ , and is consistent with either the absence of W-exchange or the exact cancellation of amplitudes expected under SU(3).

#### Cabibbo Suppressed Decays

The Cabibbo suppressed two-body decays are simplest to address experimentally. The problem of  $K \rightarrow \pi$  misidentification from the more prevalent non-suppressed channels must be treated by displaying both the signal and background in the same plot. To analyze the two channels  $D^+ \rightarrow K^+ K^-$  and  $D^+ \rightarrow \pi^+ \pi^-$ , oppositely charged pairs of tracks with the correct TOF identity are selected. To reduce non- $D$  backgrounds each pair of particles is required to have total momentum within 50 MeV of the expected momentum. The sidebands  $60 \text{ MeV} < |\delta P_T| < 110 \text{ MeV}$  provide a sample of events representing the background shape after smoothing over the whole mass region (Fig. 6). The shape so determined, accurately reproduces the regions outside the  $D$  mass. The misidentification peaks from the  $K^- \pi^+$  feeding into  $K^+ K^-$  (at  $\sim 1.968 \text{ GeV}$ ) and  $\pi^+ \pi^-$  (at  $\sim 1.740 \text{ GeV}$ ) are visible and well separated from the signals at  $1.863 \text{ GeV}$ . The number of signal events is determined by a maximum likelihood fit, fixing the mass and width of the suppressed channels, to the value measured

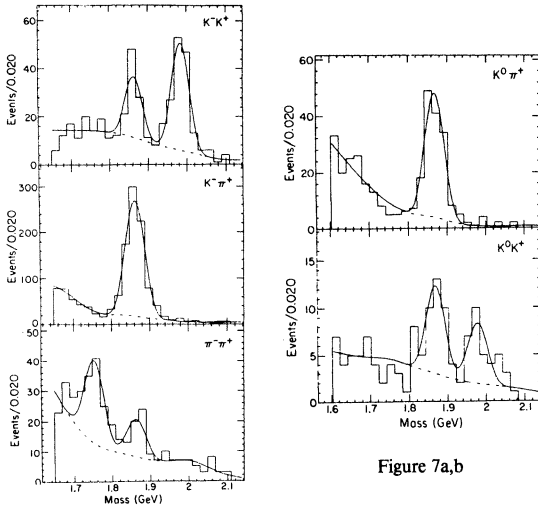


Figure 7a,b

Figure 6a-c

from the  $K^- \pi^+$  distribution. The magnitude of the background, but not its shape, is varied in the fit. We observe  $75 \pm 10 K^+ K^-$ , and  $33 \pm 9 \pi^+ \pi^-$  events. Correcting for relative efficiencies, we obtain the ratio of partial widths:

$$\Gamma(D^+ \rightarrow K^+ K^-)/\Gamma(D^+ \rightarrow K^- \pi^+) = 0.125 \pm 0.018 \pm 0.010$$

$$\Gamma(D^+ \rightarrow \pi^+ \pi^-)/\Gamma(D^+ \rightarrow K^- \pi^+) = 0.038 \pm 0.010 \pm 0.005$$

These values are in good agreement with the previous measurement of the MARK II and confirm the large deviation from exact SU(3) in the  $K^+ K^-$  case, and the smaller deviation in the  $\pi^+ \pi^-$  case. The  $\pi^+ \pi^-$  is lower than  $\tan^2 \theta_c$  by  $\sim 1$  standard deviation and the  $K^+ K^-$  is higher by  $\sim 3.3$  standard deviations, before phase space corrections ( $\sim 7\%$ ).

The same technique is applied to the decays  $D^+ \rightarrow \bar{K}^0 \pi^+$  and  $D^+ \rightarrow \bar{K}^0 K^+$  (Fig. 7). We observe  $29 \pm 6$  events in  $D^+ \rightarrow \bar{K}^0 K^+$ , yielding a ratio of partial widths:

$$\Gamma(D^+ \rightarrow \bar{K}^0 K^+)/\Gamma(D^+ \rightarrow \bar{K}^0 \pi^+) = 0.294 \pm .074 \pm .051$$

Under exact SU(3) this ratio is given:

$$\Gamma(D^+ \rightarrow \bar{K}^0 K^+)/\Gamma(D^+ \rightarrow \bar{K}^0 \pi^+) = |C|^2/|A+B|^2 \times \tan^2(\theta_c)$$

Here  $C$  is the third of the invariant amplitudes for two-body decays. From the discussion of the decay  $D^+ \rightarrow \bar{K}^0 \pi^+$ , under similar assumptions, we know  $|A| \sim |B|$ . This suggests that in the absence of SU(3) violations, either  $|C|$  must be large, or  $A$  and  $B$  amplitudes undergo a partial cancellation. Alternatively, we may be seeing the effects of SU(3) breaking, as in the case of  $D^+ \rightarrow K^+ K^-$ .

The same technique is applied to the three-body decays  $D^+ \rightarrow K^- K^+ \pi^+$  and  $D^+ \rightarrow \pi^+ \pi^+ \pi^-$ . The latter decay requires a cut on  $M_{\pi^+ \pi^-}$  to avoid accepting the non-suppressed decay of the  $D^+ \rightarrow \bar{K}_s^0 \pi^+$  where  $\bar{K}_s^0 \rightarrow \pi^+ \pi^-$ . The fit to background and signal (Fig. 8) yields  $60.5 \pm 13.0$  events in the  $K^+ K^- \pi^+$  channel, and  $70.0 \pm 18.7$  events in the  $\pi^+ \pi^+ \pi^-$  channel. As before, masses and widths have been fixed to that of the non-suppressed channel  $D^+ \rightarrow K^- \pi^+ \pi^+$ .

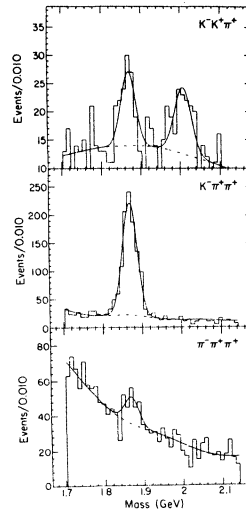


Figure 8a-c

The  $D^+ \rightarrow K^- K^+ \pi^+$  decay can be further studied for evidence of a quasi two-body pseudoscalar-vector content. We find  $18 \pm 5$  events arising from  $D^+ \rightarrow \phi^+ \pi^+$  (Fig. 9). Correcting for efficiency, we obtain:

$$\Gamma(D^+ \rightarrow K^- K^+ \pi^+)/\Gamma(D^+ \rightarrow K^- \pi^+ \pi^+) = .072 \pm .024 \pm .015$$

$$\Gamma(D^+ \rightarrow \pi^+ \pi^+ \pi^-)/\Gamma(D^+ \rightarrow K^- \pi^+ \pi^+) = .059 \pm .016 \pm .010$$

$$\Gamma(D^+ \rightarrow \phi^+ \pi^+)/\Gamma(D^+ \rightarrow K^- \pi^+ \pi^+) = .083 \pm .023 \pm .012$$

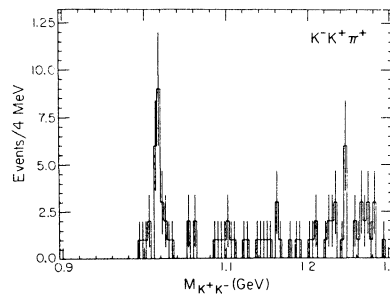


Figure 9

Here the  $\Gamma(D^+ \rightarrow K^- K^+ \pi^+)$  has the  $\phi^+ \pi^+$  subtracted and is corrected as is the decay  $D^+ \rightarrow \pi^+ \pi^+ \pi^-$ , assuming a three body phase space decay distribution. A small contribution from  $D^+ \rightarrow K^* \pi^+$  has not been subtracted. While no simple

predictions exist for the three-body decays, they do not show anomalously large partial widths relative to the typical decays like  $K^-\pi^+\pi^-$ . Our preliminary value of  $D^+ \rightarrow \phi\pi^+$  relative to  $D^+ \rightarrow K^+\rho^+$  is  $0.11 \pm .06$ . This decay is another channel which like  $D^0 \rightarrow \bar{K}^0\pi^+$ , should be color suppressed. The existence of this decay mode at this large relative rate is further evidence for the absence of color suppression in all  $D$ -decays.

#### Semileptonic Decays

The semileptonic decays of the  $D^+$  and  $D^0$  can be studied in an unambiguous manner by tagging  $D$  decays into hadronic channels where the charm of the  $D$  is uniquely determined, and searching for electrons in the tracks of the recoiling  $D$ . Three  $D^0$  ( $K^-\pi^+, K^-\pi^+\pi^-, K^-\pi^+\pi^+\pi^-$ ) and two  $D^+$  ( $\bar{K}^0\pi^+, K^-\pi^+\pi^+$ ) channels have been selected for their excellent signal to background, as tags (Fig. 2). There are  $2673 \pm 59$   $D^0$  and  $1331 \pm 41$   $D^+$  decays in the tag sample. We require tracks recoiling from the tag to have  $p > 150$  MeV, to reconstruct within 2 cm of the primary vertex, and to extrapolate to the TOF and shower counter. We remove all tracks identified by TOF as charged kaons, as well as oppositely charged tracks which have opening angles consistent with coming from a gamma conversion. Non-separable overlapping tracks in the TOF or shower counter are also removed. The remaining tracks are a mixture of pions and leptons. These are classified as pions or electrons by an algorithm utilizing their momentum, TOF, shower energy, and longitudinal and transverse shower development. The procedure is adjusted using samples of electrons from radiative Bhabba's, and pions from decays of  $K_s^0$ , and  $\Psi \rightarrow \pi^+\pi^-\pi^0$ .

The misidentification rate for pions to be called electrons is checked within the  $\Psi(3770)$  dataset independently using inclusive  $K_s^0$ . With  $\sim 85\%$  electron efficiency, this rate is  $< 3.8\%$  for pions with momentum between 1.10 and 1.100 GeV.

At each momentum, the identity of tracks having the expected lepton charge (known from the strangeness of the tagged  $D$ ) is unfolded using the measured misidentification rates. This technique takes into account the charge asymmetries in the hadronic  $D$  decays in a model independent way. The number of incorrectly charged electrons is also determined. The electrons in the latter sample provide a direct measure of the remaining QED background from gamma conversions and Dalitz decays. Small corrections are made for tag misidentification. Table IV summarizes the number of corrected tracks. Figure 10 shows the momentum distribution of electrons after correcting for  $\pi^+ \rightarrow e^+\pi^0$  misidentification.

TABLE IV

Tag	# Tags	Correct Charge Electrons	Incorrect Charge Electrons	Non- $D$ Background Electrons	Net Signal Electrons
$D^0$	$2673 \pm 59$	109.5	21.7	2.5	$85 \pm 19$
$D^+$	$1331 \pm 41$	128.7	4.4	4.1	$120 \pm 18$

The relative acceptance for  $D^0$  and  $D^+$  is  $.99 \pm .03$ , approximately independent of the  $K^*$  and  $K$  fraction of the  $D$  decay. Our preliminary value for the ratio of semileptonic branching fractions is:

$$\frac{Br(D^+ \rightarrow e^+X)}{Br(D^0 \rightarrow e^+X)} = \frac{\Gamma(D^+ \rightarrow e^+X)/\Gamma(D^+ \rightarrow \text{all})}{\Gamma(D^0 \rightarrow e^+X)/\Gamma(D^0 \rightarrow \text{all})} = 2.8^{+0.9}_{-0.6} \pm 0.3$$

Because these decays are  $\Delta I = 0$ , the partial widths for the semileptonic  $D^0$  and  $D^+$  decay should be nearly identical unless Cabibbo suppressed non-spectator

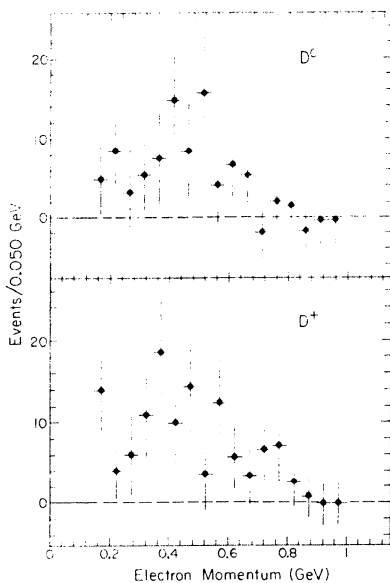


Figure 10a,b

processes in the  $D^+$  are important.<sup>[14]</sup> Thus, the ratio is actually a measure of the ratio of total widths, or the relative lifetimes of the  $D^+$  and  $D^0$ . By forming a ratio, this measurement is largely insensitive to systematic errors.

Preliminary semileptonic branching ratios for the  $D^0$  and  $D^+$  can be calculated, correcting for acceptance:

$$Br(D^0 \rightarrow e^+X) = 0.06 \pm 0.02 \pm 0.02$$

$$Br(D^+ \rightarrow e^+X) = 0.17 \pm 0.03 \pm 0.03$$

Our results indicate a somewhat larger value than the world average for the ratio of lifetimes, although the technique and systematics are quite different. The individual branching ratios are consistent with previous measurements.<sup>[13]</sup>

#### Conclusion

In trying to construct a clearer picture of the  $D$  decay mechanism, several conclusions can be drawn from the data.

The observation of both  $D^0 \rightarrow \bar{K}^0\pi^0$  and  $D^+ \rightarrow \phi\pi^+$  strongly suggests the absence of color suppression, and favors the interpretation that soft gluons, rather than W-exchange dominance, act in both cases to remove the suppression.

The  $D^+$ , having a  $\sim 17\%$  semileptonic branching ratio, is close to the expectations of a QCD corrected spectator decay with finite quark masses. The large value of the  $D^+ \rightarrow \bar{K}^0K^+$  relative to  $\bar{K}^0\pi^+$  suggests the presence of interference effects in the  $D^+$ , which may be contributing to a reduced non-leptonic width. The three-body Cabibbo suppressed  $D^+$  decays do not show a significant enhancement.

The  $D^0$  having a  $\sim 6\%$  semileptonic branching ratio, suggests that it is subject to a source of non-leptonic enhancement. The origin of the enhancement is unclear, as we are unable to observe (or rule out) a contribution from non-spectator diagrams, through limits on  $D^0 \rightarrow K^0\phi$  and  $D^0 \rightarrow K^0\bar{K}^0$ .

The high statistics measurement confirming the inequality of the branching ratios for  $D^+ \rightarrow K^+K^-$  and  $D^0 \rightarrow \pi^+\pi^-$ , along with the long  $b$  lifetime, suggests that the difference does not originate in the weak mixing angles, but rather in SU(3) violations.

#### References

- 1) R. Klanner, Proceedings of the XII Int. Conf. on High Energy Physics, Leipzig, East Germany, 1984.
- 2) R. H. Schindler et al., Phys. Rev. D24, 78 (1981).
- 3) G. S. Abrams et al., Phys. Rev. Lett. 43, 481 (1979).
- 4) J. Ellis, M. K. Gaillard and D. V. Nanopoulos, Nucl. Phys. B100, 313 (1975).
- 5) S. P. Rosen, Phys. Rev. Lett. 44, 4 (1980); S. Guberina et al., Phys. Lett. 89B, 111 (1979).
- 6) I. Bigi and L. Stodolsky, SLAC-PUB-2410 (1979).
- 7) M. Bander, D. Silverman and A. Soni, Phys. Rev. Lett. 44, 7 (1980); H. Fritzsch and P. Minkowski, Phys. Lett. 90B, 455 (1980).
- 8) I. I. Y. Bigi and M. Fukugita, Phys. Lett. 91B, 121 (1980).
- 9) M. Einhorn and C. Quigg, Phys. Rev. D12, 2015 (1975); R. Kingsley, S. Treiman, F. Wilczek and A. Zee, Phys. Rev. D11, 1919 (1975).
- 10) P. A. Rapidis et al., Phys. Rev. Lett. 39, 526 (1977); W. Bacino et al., Phys. Rev. Lett. 40, 671 (1978); R. H. Schindler et al., Phys. Rev. D21, 2716 (1980); H. Sadrozinski, XX<sup>th</sup> Int. Conf. on High Energy Physics, Madison, Wisconsin, July 1980.
- 11) D. Bernstein et al., SLAC-PUB-3222 (1983).
- 12) I. Peruzzi et al., Phys. Rev. Lett. 39, 1301 (1977); D. L. Sharre, Phys. Rev. Lett. 40, 74 (1978).
- 13) W. Bacino et al., Phys. Rev. Lett. 43, 1073 (1979); J. Feller et al., Phys. Rev. Lett. 40, 374 (1978); R. Schindler et al., SLAC Report 219 (1979).
- 14) U. Bauer and H. Fritzsch, Phys. Lett. 109B, 402 (1982).

#### Figures

- 1a) Spectator graphs for  $D^0$  and  $D^+$ . b) W-exchange graph for  $D^0$ .
- 2) Decays of the  $D^0$  and  $D^+$  to hadronic final states.
- 3a) Scatter plot of tagged  $D^0 \rightarrow K^-\pi^+$  versus  $D^0 \rightarrow K^+\pi^-$ .  
b) Scatter plot of tagged  $D^+ \rightarrow \bar{K}^0\pi^+$  versus  $D^+ \rightarrow K^+\pi^-$ .
- 4) Decay of the  $D^0 \rightarrow \bar{K}^0\pi^0$ .
- 5a)  $M_{K^*K^*}$  for  $|\delta P_D| < 50$  MeV. b)  $M_{K^*K^*}$  versus  $M_{K^*K^-}$ .
- 6)  $M_{K^*K^*}, M_{K^*\pi^+}, M_{\pi^+\pi^+}$  for  $|\delta P_D| < 50$  MeV.
- 7)  $M_{K^*K^*}, M_{K^*K^-}$  for  $|\delta P_D| < 50$  MeV.
- 8)  $M_{K^*K^*}, M_{K^*\pi^+}, M_{\pi^+\pi^+}$  for  $|\delta P_D| < 50$  MeV.
- 9)  $M_{K^*K^*}$  in  $D^+ \rightarrow K^+K^+\pi^+$ .
- 10a) Electrons from  $D^+$  decays (background subtracted)  
b) Electrons from  $D^0$  decays (background subtracted)